ACS Catalysis

Letter

pubs.acs.org/acscatalysis

Transition Metal versus Heavy Metal Synergy in Selective Catalytic Oxidations

Matthew E. Potter, A. James Paterson, and Robert Raja*

School of Chemistry, University of Southampton, Highfield, Southampton, SO17 1BJ, United Kingdom

Supporting Information

ABSTRACT: Simultaneous framework incorporation of heavy metal ions such as Ru(III) and Sn(IV) into aluminophosphate architectures generates novel bimetallic active sites, which facilitate synergistic interactions, affording high degrees of selectivity and activity in the catalytic oxidations as compared with analogous bimetallic systems, in which transition metals, such as Co(III) and Ti(IV), have been similarly incorporated.

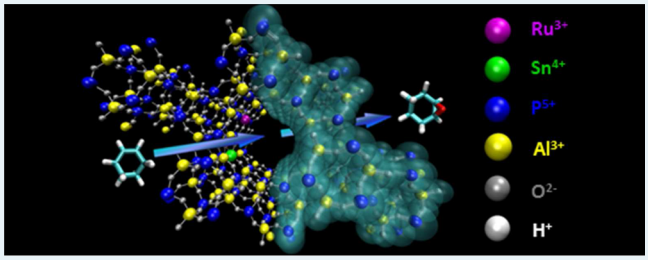

KEYWORDS: *catalytic synergy, oxidation, microporous solids, redox catalysts, multifunctional active sites*

Transition-metal-containing microporous aluminophosphate (AlPO) catalysts, wherein a few atom percent of the Al(III) or P(V) cations have been substituted with monometallic redox-active centers such as Co(III), Mn(III), Fe(III), and Ti(IV) have proved effective in catalyzing the selective oxidation of hydrocarbons and aromatics.[1−4] In marked contrast, there have been very few reports detailing the incorporation of heavy metals, such as Ru and Sn, as substituents for Al(III) or P(V) in AlPO frameworks. The use of homogeneous ruthenium-based catalysts for selective oxidation reactions has been reported,[5−7] yet there has been very little success in terms of incorporating Ru into microporous frameworks owing to the large amount of structural distortion necessary to accommodate it and its reluctance to adopt a tetrahedral geometry.

Supported Ru(III) complexes have emerged as viable catalysts for oxidation reactions, punctuated by their use in the aerobic oxidation of alcohols to ketones.[8] In marked contrast, Ru(0) active sites anchored on high-area surfaces have generated significant interest as feasible alternatives to Re and Pt for hydrogenation processes.[9] Very few examples of heterogeneous bimetallic ruthenium catalysts exist: tin-containing tetraruthenium cluster complexes,[10] hexaruthenium carbide clusters containing tin,[11] and RuSnB clusters[12] have been reported, in which the oxophilicity of tin facilitates the selective hydrogenation of polyenes, dimethyl terephthalate, and fatty acid esters. Tin has been widely used[13] as a promoter in heterogeneous catalysis and, when alloyed with ruthenium, it has been shown to greatly improve selectivity in chemical transformations.[14,15] In addition, it has been shown that both selectivity and activity of ruthenium active sites supported on γ-alumina can be suitably improved by adding tin[16] in the hydrogenation of cinnamaldehye. This improvement can be attributed to the tin sites' polarizing the carbonyl bonds, thereby facilitating Ru−H hydride transfers.

Tin-containing zeolites have also been employed as successful catalysts in their own right, showing significant activity in Baeyer−Villiger oxidations[17] and MPVO rearrangements.[18] The activity of these catalysts in these oxidation reactions does not stem from its redox capability, but from the ability of the oxophilic tetrahedral tin to alter the polarization in C−O bonds via Sn−O interactions, thereby facilitating hydride transfers. It was concluded from these studies that these interactions make Sn(IV) a more effective substituent than Ti(IV) in framework structures, such as AlPO's, for effecting these catalytic processes. There are numerous reports[19,20] in the literature detailing the effectiveness of Ti(IV)-containing porous solids, such as TS-1 and Ti-MCM-41, for oxidations in general and epoxidation in particular, but the role of isomorphously substituted Sn(IV) ions in porous architectures and its concomitant interactions with other isomorphously substituted heavy metals in the immediate vicinity remains comparatively unexplored.

Although there have been numerous examples in the literature in which Ru has been deposited, anchored, or ion-exchanged onto solid supports as Ru(III)[8] or Ru(0),[9] to the best of our knowledge, our study reveals, for the first time, the successful framework incorporation of ruthenium into an AlPO framework. Furthermore, the simultaneous incorporation of Sn(IV), as an isomorphous replacement for P(V) within this bimetallic catalytic system, confers considerable synergistic enhancements in catalytic potential compared with other recently reported transition-metal-containing bimetallic catalysts[21] in the selective epoxidation of olefins.

In this study, we have focused on the incorporation of Zn(II), Ru(III), and Sn(IV) ions into the AlPO-5 framework.

Received: June 22, 2012
Revised: September 21, 2012
Published: October 19, 2012

The contrasting chemistry, ionic size, and intended framework substitution positions make these metals good candidates for initiating synergistic interactions. It is believed that Zn-containing solids are not very effective in facilitating oxidation reactions, as attributed to their ability to readily form ZnO phases,[22] but nevertheless, their effectiveness as solid-acid catalysts in the dehydration of propylene glycol and in the rearrangement of α-pinene oxide[23,24] has been reported. There have been very few reports in the literature that conclusively demonstrate the incorporation of Zn into an AFI framework. By using our preparative methodology (see Supporting Information, page S3), we have also confirmed that it is indeed difficult to substitute Zn into the AlPO-5 framework. As such, aggregates and ZnO phases are formed,[22] instead of isolated, tetrahedrally substituted framework Zn sites, resulting in lower surface areas (Table 1) and less-crystalline XRD patterns.

Table 1. ICP and Surface Area Measurements of Ru/Sn/ZnAlPO-5 Catalysts

	ICP metal loading/wt%			
	Ru	Sn	Zn	BET surface area/m^2 g^{-1}
AlPO-5				295
RuAlPO-5	2.90			282
RuSnAlPO-5	1.42	2.33		328
SnAlPO-5		4.22		268
ZnAlPO-5			3.35	165
SnZnAlPO-5		2.16	0.96	280
RuZnAlPO-5	1.85		1.54	341
RuSnZnAlPO-5	1.22	1.94	0.97	250
Ru/AlPO-5[a]	0.84			129
Sn/AlPO-5[a]		2.87		169
RuSn/AlPO-5[a]	0.82	2.60		154

[a]Samples prepared by wet impregnation; see SI Table S2 for further details.

Details of the synthetic procedures for the monometallic, bimetallic, and trimetallic AlPO's containing Ru, Zn, and Sn are given in the Supporting Information (SI) (denoted as MAlPO-5, see Table S1). The structure-directing agent, *N*,*N*-methyldicyclohexylamine, used in our synthesis is known to have a high affinity for the AFI structure,[25] and it has been proposed that it is possible to incorporate heavier metals into the framework architectures because the structure-directing agent may permit the creation of small defects to preserve the overall AFI structure. For the purpose of comparison and to contrast differences in the incorporation of the metal ions, we have also synthesized monometallic and bimetallic Ru/Sn catalysts using a wet impregnation approach,[26] as outlined in the experimental section (see Supporting Information, page S4 and Table S2).

Inductively coupled plasma (ICP-MS) results confirmed the presence of the intended quantities of metal ions in the calcined materials (Table 1 and SI Table S4). The ICP-MS results further reveal a linear relationship between the quantity of ruthenium added to the gel during synthesis and the ruthenium content of the final calcined product. The linear trend that was obtained (for the Ru) coupled with the level of tolerance that was reflected for the other elements (Al, P) in the final product strongly indicates the incorporation of the heavy metals into the framework. If the ruthenium was located in extra-framework sites, there would be a strong deviation from this linear trend (Figure 1), resulting in a sharp cutoff that would be indicative

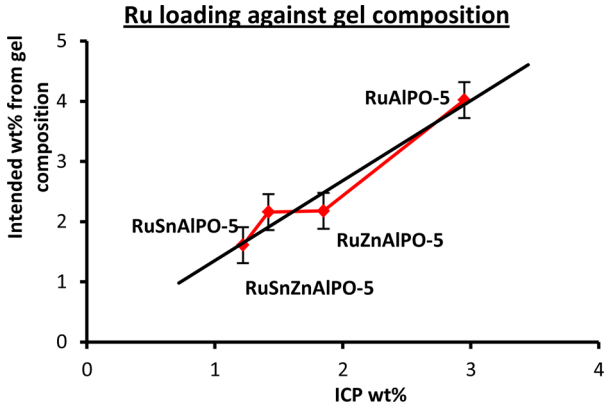

Figure 1. Plot of Ru loading (from ICP; wt %) versus intended framework incorporation from gel composition (for analogous Sn and Zn experimental plots, see Supporting Information Figures S11 and S12).

of clustering of the ruthenium species, as observed in the samples prepared by wet impregnation. We also note that the ruthenium content in the samples prepared by wet impregnation is significantly lower than intended (in marked contrast with the framework-incorporated catalysts), which could be attributed to the removal of weakly bound physisorbed ruthenium species by washing. Furthermore, we observe a constant Al/P ratio for the catalysts prepared by wet impregnation (as expected), whereas we see a deviation from this value (SI Table S4) for the Ru and Sn samples prepared by our framework-incorporation route, which further substantiates the incorporation of the metal ions into the framework of the AFI architecture.

Typical powder XRD patterns for the framework-incorporated calcined monometallic Ru(III)AlPO-5 and Sn(IV)AlPO-5 and the corresponding bimetallic analogue, Ru(III)Sn(IV)-AlPO-5, are shown in Figure 2 (see also SI Figures S4–S9).

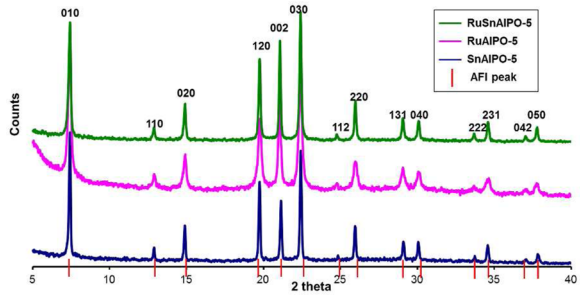

Figure 2. Powder X-ray diffraction patterns for the monometallic and bimetallic AlPO's containing Ru and Sn.

The indexed patterns of the samples are in good agreement with that reported in the literature for the AFI structure,[27] with only a minimal distortion of the AFI unit cell (see SI Table S3). Given the relatively low levels of incorporation of ruthenium and tin (see sample composition from ICP results; SI Table S4), our calculations (see SI pages S14–S15) further confirm that the loadings we have employed would have minimal effect on the unit cell size and dimensions.[28] All observable peaks can be attributed to the AFI structure; therefore, it can be concluded that there are no phase impurities present. The crystallinity of the materials was found to significantly increase on calcination, a characteristic particularly observed with the

dx.doi.org/10.1021/cs300404u | *ACS Catal.* 2012, 2, 2446–2451

ruthenium-based catalysts (SI Figure S9). In contrast, the ZnAlPO-5 catalyst afforded lower surface areas (Table 1) and less-crystalline XRD patterns (SI Figure S5), owing to the formation of aggregates and ZnO phases,[22] instead of isolated, tetrahedrally substituted framework Zn sites. Powder XRD of the samples prepared by wet impregnation (SI Figure S10) confirms that the AFI framework is intact and stable after the second calcination, and secondary structural phases were not detected (SI Figure S10).

Scanning electron microscopy (SEM; SI Figures S16–S21) on the calcined framework-incorporated monometallic and bimetallic samples revealed a particle morphology and mean particle sizes that were consistent with that reported in the literature.[29] The SEM micrographs exclusively showed spherical particles with diameters between 10 and 20 μm, further indicating the phase purity, crystallinity, and uniformity of the samples. In contrast, the SEM images of the samples prepared by wet impregnation displayed analogous particle morphology but were conspicuous with the presence of large agglomerates and aggregates (SI Figures S22–S25). It was also noteworthy that these samples displayed a lower surface area (Table 1), with the metal ions prominently located in extra-framework sites due to the formation of metal oxide agglomerates, as indicated from preliminary microscopy studies and EDX data (SI Table S5), in stark contrast to the Ru and Sn catalysts prepared by framework incorporation.

Volumetric analyses further confirmed the porous nature of the materials, with all samples possessing surface areas that are consistent with that of the undoped AlPO-5 sample. BET measurements revealed that the surface areas of RuAlPO-5, SnAlPO-5, and RuSnAlPO-5 are comparable (282, 268, and 328 $m^2\ g^{-1}$, respectively) and show little variation from the value for metal-free AlPO-5 (295 $m^2\ g^{-1}$). The slight variation in surface area for the framework-incorporated AlPO's can be attributed to minor structural distortions that might have emerged on incorporating a larger metal ion substituent into the framework. The good agreement observed between the RuSnAlPO-5 and the metal-free AlPO-5 again suggests that the pores of the RuSnAlPO-5 are clear and free of adsorbed clusters.

In contrast, the Ru and Sn catalysts prepared by wet impregnation show a dramatic decrease in surface area, despite the lower loadings of metal present, when compared with their framework-incorporated counterparts. The preparative methodology has predominantly resulted in secondary phases and metal oxide aggregates, which contribute to the lower surface area (and catalytic activity/selectivity; see below). On the other hand, the Ru and Sn catalysts prepared by hydrothermal framework incorporation show no signs of extraframework speciation, which could, in part, be responsible for the relatively higher surface areas.

Owing to their intense color, it is inherently difficult to characterize ruthenium-containing catalysts using conventional spectroscopic techniques. However, limited information on the nature of the Ru active site can be gained using magnetic resonance techniques.[30,31] Electron paramagnetic resonance (EPR) provides good insights into the oxidation states of the framework-substituted metal ions because Ru(III) is paramagnetic and EPR-active, whereas diamagnetic Zn(II) and Sn(IV) are EPR-silent. A typical EPR spectrum obtained for Ru(III) in mono-, bi-, and trimetallic AlPO-5 frameworks showed a single, sharp peak, indicative of discrete, isolated sites, with very little evidence of metal–metal interactions through metal sintering or ruthenium clustering. The position of the EPR peak (see SI Figures S13–S15) was located at 3440 gauss in all ruthenium-containing samples, equating to a g value of 2.058. This value is in good agreement with that found in the literature[32] for low-spin Ru(III) ions in zeolitic frameworks and also framework-incorporated heteropolyanion and polyoxometalate species.[33,34] Given that previously observed and reported g values for Ru(III) ions in zeolites beta, Y, and ZSM-5 are in good agreement[32] with our calculated values (see SI Table S6), we can conclude that the ruthenium ions in all our samples are present as Ru(III) in a low-spin state and possess multiple bonds to framework oxygen ions, thus confirming framework incorporation. No other peaks were observed in the EPR spectrum, further confirming that there were no other paramagnetic species associated with the framework, in line with our expectations. The agreement of our g values to analogous Ru(III)-containing zeolitic systems coupled with the sharp spectral feature observed in our samples further indicates that it is highly likely that a majority of the Ru(III) ions are present in the material as isolated single-site entities. Given the above, we believe that the synthesis procedures that we have evolved and the design strategies that we have employed have resulted in the incorporation of the Ru and Sn in the AFI system.

The catalytic data for the epoxidation of cyclohexene, employing acetylperoxyborate (APB)[35] as the oxidant, for the mono-, bi-, and trimetallic samples is summarized in Figure 3,

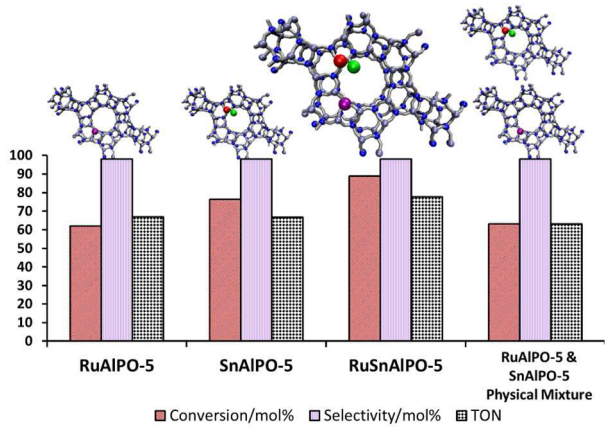

Figure 3. Comparison of catalytic performance with monometallic and bimetallic Ru–Sn catalysts. See Table 2 for reaction conditions.

Table 2 and SI Table S7 (with good mass balance). It can be seen that all catalysts achieved a reasonable level of conversion (>60%) and a high selectivity (>98%). However, on closer introspection of the turnover numbers (TON), it is clear that

Table 2. Influence of Zn Species in Epoxidation of Olefins[a]

catalyst	conversion/mol %	TON
ZnAlPO-5	72.6	40.5
RuZnAlPO-5	64.1	43.8
SnZnAlPO-5	75.1	53.2
RuSnZnAlPO-5	69.3	46.4

[a]Reaction conditions: 7 mL of DCM, 3.0 mmol of cyclohexene, 100 mg of catalyst, 3.3 mmol of APB dissolved in 10 mL of H_2O, refluxed at 66 °C, calibrated with triglyme internal standard (SIFigure S1–S3). Selectivity >98% in all cases.

dx.doi.org/10.1021/cs300404u | ACS Catal. 2012, 2, 2446–2451

despite the seemingly good conversions, the monometallic ZnAlPO-5 is considerably less active than the monometallic RuAlPO-5 or SnAlPO-5 species (in terms of catalytic turnovers; see Figure 3). This suggests that the heavier metal substituents have a greater affinity for this catalytic oxidation than the zinc-containing analogue. This trend is more conspicuous by the fact that every zinc-containing catalyst has a lower TON when compared with its equivalent zinc-free analogue. This further demonstrates that not only are Zn active centers comparatively less efficient for this catalytic oxidation, but they are also actively hindering the effectiveness of the catalyst when incorporated with other metals in the multimetallic catalysts (Table 2).

Although it could be argued that the lower surface area afforded by the ZnAlPO-5 (165 $m^2 g^{-1}$) could be a mitigating factor for the observed lower TONs, it is difficult to rationalize the catalytic performance solely on surface properties because the RuZnAlPO-5 has, in effect, twice the surface area (341 $m^2 g^{-1}$) when compared with the ZnAlPO analogue, yet it affords a similar TON. This also rules out the possibility of any diffusion limitations affecting the former catalyst. Given the relatively moderate conversions and uniform selectivities achieved with ZnAlPO-5, it is highly unlikely that the zinc sites are, in parallel, decomposing the reactant or oxidant, because this would have resulted in lower conversions and inferior product selectivity. In light of the above, it has been proposed that the inferior performance of the zinc-containing catalysts can be attributed to metal itself or its propensity for forming extra-framework species that could be associated with the formation of a ZnO phase that have a deleterious effect on the ensuing catalysis, a justified conclusion when contrasting the related chemistries associated with the incorporation of Ru, Sn, and Zn in the aluminophosphate material. Because of the acidic nature of ZnAlPO's (owing to the Brønsted acid sites that are present), it has been suggested that, the active site binds strongly to the oxidant through enhanced hydrogen bonding. This would, in turn, impede the propensity of the oxidant from binding to other reactive active sites (Ru or Sn) in the corresponding multimetallic catalysts, thereby hindering their reactivity (Table 2) but, more importantly, weaken any prospects for evoking catalytic synergy associated these multimetallic substitutions.[21]

In marked contrast, the monometallic RuAlPO-5 and SnAlPO-5 catalysts display an enhanced catalytic performance with TONs of 66.8 and 66.6, respectively, when compared with the analogous ZnAlPO-5 catalyst (TON of 40.5). Interestingly, when both metals are incorporated into the AlPO-5 framework (to afford a bimetallic RuSnAlPO-5 catalyst), both the conversion (88.9%) and TON (77.6) are significantly increased. It is noteworthy that the enhancements in catalytic behavior, when comparing the monometallic RuAlPO-5 and SnAlPO-5 catalysts with the bimetallic RuSnAlPO-5 analogue, are in good agreement with the physicochemical and preliminary structural characterization (discussed earlier), suggesting that the significant increase in observed catalytic TONs is not due to any physical differences between the samples. It is therefore believed that the observed improved enhancement in catalytic performance can be attributed to the synergistic interaction between the two individual metals (Ru and Sn).

To further validate the above observation, a physical mixture of RuAlPO-5 and SnAlPO-5 (containing moles of individual monometal composition identical to that of the RuSnAlPO-5 catalyst) was prepared and tested under analogous reaction conditions to probe the origin of the catalytic synergy (Figure 3). The TONs obtained with this physical mixture were comparable to that obtained with the individual monometallic catalysts, which further confirms that the enhanced activity with the bimetallic catalyst does not simply arise by having two monometallic analogues in the same reaction mixture, but to engineer the observed synergy, both metals must be incorporated within the same framework architecture. It is now apparent that not only does the ability to facilitate catalytic synergy rely on the location and distribution of the individual metal ions within the framework but also the proximity of the two metals could play a pivotal role in enhancing the catalytic turnover.[6,21] Remarkably, the bimetallic Ru−Sn catalyst prepared by the wet impregnation approach and the physical mixture of the corresponding monometallic analogues did not reveal any significant enhancements in catalytic synergy when compared with equivalent catalysts prepared by the framework-incorporation method (SI Table S7). This clearly illustrates that the synergistic effect that we have observed can be directly attributable to the simultaneous incorporation of both the metal ions into the AFI framework. In addition, it is also important to encompass appropriate metal combinations (with a judicious choice of transition metal versus heavy metal; see below), on the basis of their inherent chemical properties, for effecting the desired outcome within the targeted reaction.

In our previous work,[21] we have demonstrated that the simultaneous isomorphous substitution of Al(III) and P(V) sites with transition metals such as Co(III) and Ti(IV) affords synergistic enhancements in catalytic oxidation reactions. In this work, we have specifically focused on analogous heavy metal substitutions within the same framework architecture (AFI) for facilitating meaningful comparisons with the former. Although the individual monometallic RuAlPO-5 and SnAlPO-5 systems far surpass the catalytic performance of the previously reported[21] CoAlPO-5 and TiAlPO-5 catalysts, it was again remarkable that the TONs obtained with bimetallic RuSnAlPO-5 far exceed the performance of the corresponding bimetallic CoTiAlPO-5 analogue (Figure 4). The propensity of the heavy metal substituents to far outweigh the performance of the corresponding transition metal analogues, in both the monometallic and bimetallic catalysts, has again demonstrated a synergy between a M(III) and M(IV) site. It is also noteworthy that the TONs obtained here with the heavy metal

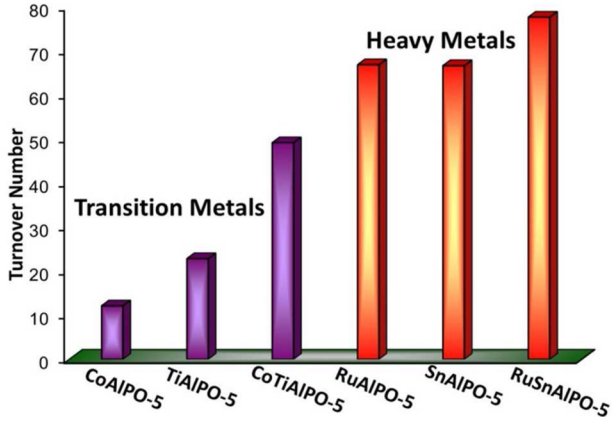

Figure 4. Contrasting synergistic effects in catalytic performance between framework-incorporated transition metals and heavy metals. See Table 2 for reaction conditions.

dx.doi.org/10.1021/cs300404u | ACS Catal. 2012, 2, 2446−2451

substituents far exceed the catalytic performance of our previously reported[21] Co/TiAlPO series.

The heterogeneous nature of all catalysts and that of the RuSnAlPO-5 in particular was scrutinized carefully by running catalyst recycle tests in triplicate (SI Figure S26), in accordance with stringent procedures and hot-filtration experiments that have been described earlier.[36] No appreciable loss in catalytic activity was observed, and detailed analyses of the reaction mixtures revealed less than 5 ppb of ruthenium and 2 ppb of tin (by MP-AES), further confirming that no significant deactivation of the active sites (by aggregation or sintering) or leaching occurs during catalysis.

In summary, we have found that heavy metal dopants (such as Ru and Sn) in framework architectures display enhanced catalytic turnovers when compared with their corresponding transition metal analogues (such as Co and Ti) in selective oxidation reactions. In particular, the bimetallic analogues of the former exhibit a concomitant enhancement in catalytic potential when compared with the corresponding bimetallic transition metal counterparts, suggesting a synergistic enhancement in catalytic properties (SI Figure S30). The synthetic strategy that we have evolved (SI Figure S27), coupled with the preliminary characterization evidence reported here, reveal that the isolated nature of the single-site entities is responsible for the enhanced catalytic activities of these catalysts. Although further information regarding the exact nature of the active site (SI Figures S28 and S29), its coordination geometry, and proximity to other active sites within the framework (SI Figure S31) will be required to afford detailed structure−property correlations (in situ X-ray absorption (EXAFS and XANES) studies are currently underway), these initial catalytic findings open up exciting prospects for expanding the scope of these catalysts to other industrially significant oxidation reactions.[37−41]

■ ASSOCIATED CONTENT

Supporting Information

Detailed experimental procedures and gel composition data for the syntheses of all catalysts, characterization techniques, and catalytic procedures are summarized. Unit cell parameters (XRD) for the monometallic and bimetallic framework-incorporated Ru- and Sn-containing catalysts have been provided along with representative SEM images and EPR spectra. Typical GC calibrations, mass balance, and catalyst recycle data are also provided. This information is available free of charge via the Internet at http://pubs.acs.org/.

■ AUTHOR INFORMATION

Corresponding Author

*Fax: (+44)-2380-593781. E-mail: R.Raja@soton.ac.uk.

Author Contributions

The manuscript was written through contributions of all authors.

Funding

Financial assistance from Honeywell LLC (USA) is gratefully acknowledged.

Notes

The authors declare no competing financial interest.

■ ACKNOWLEDGMENTS

We thank Dr. Radoslaw Kowalczyk and Dr. Lyle Monson (UOP) for their assistance with electron paramagnetic resonance and induced coupled plasma studies. Dr. Alan Levy (Honeywell) is gratefully acknowledged for many helpful discussions. We also acknowledge the RCaH for assistance with transmission electron microscopy studies.

■ REFERENCES

(1) Centi, G. Methods and Tools for Sustainable Industrial Chemistry: Catalysis. In *Sustainable Industrial Chemistry*; Centi, G., Ed.; Wiley-VCH: Weinheim, 2009; p 120.
(2) Hartmann, M.; Kevan, L. *Chem. Rev.* **1999**, *99*, 635−663.
(3) Raja, R.; Sankar, G.; Thomas, J. M. *J. Am. Chem. Soc.* **1999**, *50*, 11926−11927.
(4) Lee, S. O.; Raja, R.; Harris, K. D. M.; Thomas, J. M.; Johnson, B. F. G.; Sankar, G. *Angew. Chem., Int. Ed.* **2003**, *42*, 1520−1523.
(5) Trnka, T. M.; Grubbs, R. H. *Acc. Chem. Res.* **2001**, *34*, 18−29.
(6) Goldstein, A. S.; Beer, R. H.; Drago, R. S. *J. Am. Chem. Soc.* **1994**, *116*, 2424−2429.
(7) Vennat, M.; Bregeault, J. M. *Appl. Catal., A* **2010**, *386*, 9−15.
(8) Dijksman, A.; Marino-Gonzalez, A.; Mairati i Payeras, A.; Arends, I. W. C. E.; Sheldon, R. A. *J. Am. Chem. Soc.* **2001**, *123*, 6826−6833.
(9) Joshi, R.; Chudsama, U. *Ind. Eng. Chem. Res.* **2010**, *49*, 2543−2547.
(10) Adams, R. D.; Boswell, E. M.; Captain, B.; Hungria, A. B.; Midgely, P. A.; Raja, R.; Thomas, J. M. *Angew. Chem., Int. Ed.* **2007**, *46*, 8182−8185.
(11) Hermans, S.; Raja, R.; Thomas, J. M.; Johnson, B. F. G.; Sankar, G.; Gleeson, D. *Angew. Chem., Int. Ed.* **2001**, *40*, 1211−1216.
(12) Pouilloux, Y.; Autin, F.; Guimon, C.; Barrault, J. *J. Catal.* **1998**, *176*, 215−224.
(13) Zhu, L.; Yempally, V.; Isrow, D.; Pellechia, P. J.; Captain, B. *J. Organomet. Chem.* **2010**, *695*, 1−5.
(14) Ishii, K.; Mizukami, F.; Niwa, S.; Kutsuzawa, R.; Toba, M.; Fujii, Y. *Catal. Lett.* **1998**, *52*, 49−53.
(15) Neri, G.; Pietropaolo, R.; Galvagno, S; Milone, C.; Schwank, J. *J. Chem. Soc., Faraday Trans.* **1994**, *90*, 2803−2807.
(16) Neri, G.; Mercadante, L.; Milone, C.; Pietropaolo, R.; Galvagno, S. *J. Mol. Catal. A: Chem.* **1996**, *108*, 41−50.
(17) Corma, A.; Nemeth, L. T.; Renz, M.; Valencia, S. *Nature* **2001**, *412*, 423−425.
(18) Corma, A.; Domine, M. E.; Nemeth, L.; Valencia, S. *J. Am. Chem. Soc.* **2002**, *124*, 3194−3195.
(19) Blasco, T.; Corma, A.; Navarro, M. T.; Pariente, J. P. *J. Catal.* **1995**, *156*, 65−74.
(20) Saxton, R. J. *Top. Catal.* **1999**, *9*, 43−57.
(21) Paterson, J.; Potter, M. E.; Gianotti, E.; Raja, R. *Chem. Commun.* **2011**, *47*, 517−519.
(22) Sun, D.-L.; Deng, J.-R.; Chao, Z.-S. *Chem. Cent. J.* **2007**, *1*, 27.
(23) Wilson, K.; Rénson, A.; Clark, J. H. *Catal. Lett.* **1999**, *61*, 51−55.
(24) Dai, Z.; Hatano, B.; Tagaya, H. *App. Catal., A* **2004**, *258*, 189−193.
(25) Sanchez-Sanchez, M.; Sankar, G.; Simperler, A.; Bell, R. G.; Catlow, C. R. A.; Thomas, J. M. *Catal. Lett.* **2003**, *88*, 163−167.
(26) Da Qu, L.; Li, J.; Hao, Z.; Li, L. *Catal. Lett.* **2009**, *131*, 656−662.
(27) *Collection of simulated XRD powder patterns for Zeolites*, 5th ed.; Treacy, M. M. J., Higgins, J. B., Eds.; Elsevier Science and Technology: Oxford, 2007.
(28) Blasco, T.; Concepcion, P.; Lopez Nieto, J. M.; Perez-Pariente, J. *J. Catal.* **1995**, *152*, 1−17.
(29) Wang, J. Y.; Song, J. W.; Yin, C. Y.; Ji, Y. Y.; Zou, Y. C.; Xiao, F. S. *Microporous. Mesoporous Mater.* **2009**, *117*, 561−569.
(30) Tfouni, E.; Krieger, M.; McGarvey, B. R.; Franco, D. W. *Coord. Chem. Rev.* **2003**, *236*, 57−69.
(31) Motten, A. G.; Hanck, K.; Dearmond, M. K. *Chem. Phys. Lett.* **1981**, *79*, 541−546.
(32) Carl, P. J.; Larsen, S. C. *J. Catal.* **2000**, *196*, 352−361.
(33) Neumann, R; Abu-Gnim, C. *J. Am. Chem. Soc.* **1990**, *112*, 6025−6031.

(34) Khenkin, A. M.; Efremenko, I.; Weiner, L.; Martin, J. M. L.; Neumann, R. *Chem.—Eur. J.* **2010**, *16*, 1356−1364.
(35) Chemie GMBH; Peroxid. U.S. Patent 5462692, 1995.
(36) Raja, R.; Thomas, J. M.; Greenhill-Hooper, M.; Ley, S. V.; Paz, F. A. A. *Chem.—Eur. J.* **2008**, *14*, 2340−2348.
(37) Raja, R. U.S. Patent 2010/0249476, July 15, 2010.
(38) Raja, R.; Paterson, A. J. World Patent 2010/079324, July 15, 2010.
(39) Lefenfeld, M.; Raja, R.; Paterson, A. J.; Potter, M. E. US Patent 2010/0249476, September 30, 2010.
(40) Lefenfeld, M.; Raja, R.; Paterson, A. J.; Potter, M. E. World Patent 2010/085708, July 29, 2010.
(41) Potter, M. E.; Raja, R.; Levy, A. U.S. Patent filed 28/10/2011.